Systematics of proton absorption deduced from (p,p) and (p,n) cross sections for 2.0- to 6.7-MeV protons on ^{107,109}Ag and ^{115}In

R. L. Hershberger, D. S. Flynn, and F. Gabbard
University of Kentucky, Lexington, Kentucky 40506

C. H. Johnson
Oak Ridge National Laboratory, Oak Ridge, Tennessee 37830

(Received 6 August 1979)

The (p,p) and (p,n) cross sections were measured to accuracies of $\pm 2\%$ and $\pm 3\%$, respectively, for 2.0- to 6.7-MeV protons on ^{107,109}Ag and ^{115}In. Hauser-Feshbach calculations, which included γ-ray emission channels, were used to convert the (p,n) cross sections to proton absorption cross sections. Analysis of the (p,p) and deduced proton absorption cross sections were made simultaneously using a conventional optical-model potential. The measured cross sections can be described using parameters extrapolated from the Sn region in a systematic way, except for a large increase required for the depth of the absorptive potential.

[NUCLEAR REACTIONS ^{107,109}Ag and ^{115}In (p,p) and (p,n), $E=2.0$ to 6.7 MeV, resolution 30 to 70 keV, enriched targets. Measured $(d\sigma/d\Omega)$ (p,p) at 135° and 165°, and total $\sigma(p,n)$. Observed analog resonances. Statistical-model and optical-model analyses, deduced model parameters.]

I. INTRODUCTION

In recent years optical-model potentials[1,2] have been used to represent average properties of nuclei revealed through nuclear reaction and scattering measurements. The (p,n) reactions on nuclei in the mass 100 region, especially the Sn isotopes, have been used to observe the $3p$ single-particle resonance[3] and to determine a global optical-model potential for this energy and mass region.[4,5] Although the global potential of Ref. 4 represented their (p,n) cross sections well and, for the most part, had reasonable parameters, the depth of the absorptive potential was required to have an anomalous A dependence. This anomalous A dependence has raised several questions about the measurements and about the analysis.

To provide independent measurements of cross sections[5] in this mass region, measurements of (p,n) reactions for ^{107,109}Ag and ^{115}In have been repeated under different experimental conditions at the University of Kentucky's Van de Graaff Laboratory and have been extended to higher energies. For this to be a meaningful test, the experimental accuracy has, for the most part, been kept to $\pm 3\%$.

An objection one might raise about the analysis of Johnson *et al.*[5] and their conclusion that the imaginary potential has an anomalous behavior in the $A=100$ mass region is that only the proton absorption cross section was used as a data base to derive the optical-model potential parameters. To remove this possible objection in the present work, the elastic scattering cross sections have also been measured and are presented as the ratio of the measured cross sections to the Rutherford scattering cross section. The $(d\sigma/d\Omega)(p,p)$ were measured as a function of proton energy at two angles to an accuracy of approximately $\pm 2\%$ and have been fitted together with the $\sigma(p,n)$ data in order to derive a consistent optical-model potential.

Although isobaric analog resonances were observed in the Ag measurements at energies which agree with those from previous experiments,[6] the present analysis did not include them. Inclusion of the isobaric analog resonances would not have had an important effect on the optical-model parameters derived here.[7]

II. EXPERIMENTAL METHOD

A. Proton beam

Protons produced by a High Voltage Engineering Corp. (HVEC) 6.5-MV CN electrostatic accelerator were analyzed by a 90° magnet. The magnet was calibrated, including relativistic corrections, using the ^{7}Li(p,n) and ^{27}Al(p,n) thresholds at 1879.13 ± 0.06 keV and 5798.5 ± 1.3 keV, respectively.[8] The proton beam energy was determined to $\pm 0.1\%$ with a beam energy spread of less than 2 keV at full width at half maximum (FWHM).

The energy of the protons in the target was assumed to depend linearly on the stopping power times the distance into the target. The proton energy corresponding to the resulting measured

average cross section was taken to be the cross section weighted average of all proton energies within the target.

The number of incident protons passing through the target was determined by integrating the beam current to obtain the total charge deposited in the Faraday cup. The precision of the current integration system was determined to be ±0.2%. The system was checked repeatedly with a precision current source.

B. Proton scattering chamber

The (p,p) cross sections were measured in a precision 30 cm diameter scattering chamber.[9] The incident beam was collimated to 1.5 mm diameter by a 31 cm long collimating assembly. The beam charge was collected in a Faraday cup with electron suppression. Beam loss due to small angle scattering was calculated to be negligible for the energies and target thicknesses used. Zero target angle was checked for each target by measuring the yield as a function of target angle. Detector angle and subtended solid angle were checked by rotating the detectors through the same series of observation angles and comparing yields. Each detector was collimated and subtended a solid angle at the target of 0.371 msr. Measuring yields as a function of beam intensity gave a dead time correction of 2.0% per 1000 counts/sec. Counting rates were normally kept below 500 counts/sec so that the dead time correction was less than 1%.

C. Neutron detection

Neutrons from the (p,n) reactions were counted using the University of Kentucky's 4π neutron detector.[10] The detector consists of a 60 cm diameter polyethylene sphere in which eight $^{10}BF_3$ counters are embedded. The Faraday cup consists of the beam pipe into and out of the sphere, the target chamber, and the beam dump which stopped the beam 2.5 m from the target. The sphere was shielded from the accelerator, analyzing magnet, and beam dump by paraffin and concrete block walls. The relative detector efficiency was determined to be constant to ±2% for the neutron energy range of 30 keV to 1.5 MeV.[10] Because of various changes in the sphere since the measurements described in Ref. 10, the absolute efficiency was remeasured. It was determined to be 0.604 ±0.7% at an average neutron energy of 500 keV using the National Bureau of Standards RaBe photoneutron source, NBS-II.[11] System counting efficiency was repeatedly monitored using a PuBe neutron source. Dead time corrections were determined to be 0.2% per 1000 counts/sec. Counting rates were usually kept below 1000 counts/sec. Backgrounds were approximated by counting neutrons with the beam stopped before the target chamber and stopped by the beam dump with no target in the chamber. In addition, the background for ^{107}Ag was measured directly at low energies by going below the 2.22 MeV ^{107}Ag (p,n) threshold. These background corrections varied from ~14% at 3.5 MeV to ~0.3% at 6 MeV.

D. Targets

Special emphasis was placed on the production of highly uniform targets. All targets had nominal areal densities of 1 mg/cm^2 and were produced in vacuum by vapor deposition on glass slides coated with a thin layer of NaCl. The slide, masked to a circular area of nominally 3 cm^2, was held in an off axis geometry and rotated during evaporation. The targets, after floating off the slides and drying, were thin disks which could be weighed before mounting. The mounted targets were put into the scattering chamber to check for uniformity, to check on light mass impurities, and to get an independent measure of the target thickness by measuring (p,p) scattering yields at low energies and assuming Rutherford scattering. After measurements were completed on the ^{109}Ag target, a 1.8 cm^2 disk was punched out of the center of the target. It was then weighed, mounted, and remeasured in the scattering chamber to give a measure of the accuracy of the target thickness determination.

The ^{107}Ag and ^{109}Ag targets were enriched to 98.54% and 99.26%, respectively. The ^{115}In target was made from natural indium metal. Since ^{nat}In is 95.72% ^{115}In, the cross sections measured using a ^{nat}In target are essentially those of ^{115}In. Cross sections for the minor Ag or In isotopes in the targets were assumed to be approximately equal to the major isotope so that no correction was necesaary. The targets were inspected for impurities by observing their proton induced x-ray emission (PIXE) as well as back scattering of protons in the scattering chamber. Both methods showed that all targets were essentially free of impurities.

III. PRESENTATION OF EXPERIMENTAL DATA

Both the (p,p) and (p,n) cross sections are dominated by large and, for the purpose of the present work, uninteresting Coulomb effects. To a large extent these effects can be removed, revealing any nuclear effects which might otherwise be hidden.

The (p,n) excitation function rises nearly exponentially due to the Coulomb penetrability. How-

ever, by converting the (p,n) cross sections to averaged strength functions the nuclear effects are more directly displayed. These l-averaged experimental strength functions[12] are defined to be

$$\langle S_{p,n}\rangle \equiv R\frac{\langle\sigma_{p,n}\rangle}{4\pi^2\hbar^{-2}\sum_l(2l+1)P_l},$$

where $\langle S_{p,n}\rangle$ has units of fm, $\langle\sigma_{p,n}\rangle$ is the measured cross section, and P_l is the Coulomb penetration factor for l-wave protons at a radius $R=1.45\ A^{1/3}$ fm. The (p,n) data,[13] converted to strength functions, are presented in Fig. 1 where the zero of the ordinate scale has been suppressed in order to enhance details of the structure. For comparison, we have also included data taken by Johnson *et al.*[5] which are independent absolute measurements. In the worst case, ^{109}Ag, there is a 3.5% difference at 5.25 MeV between the two sets of data. This is within the accuracy of the two measurements. The error bars indicate counting statistical uncertainties only. One of the largest errors in the data, ~±4% at 3.5 MeV, is due to the large background correction at low energies. To facilitate the extraction of cross sections from Fig. 1, a summary of smoothed (p,n) cross sections is given in Table I.

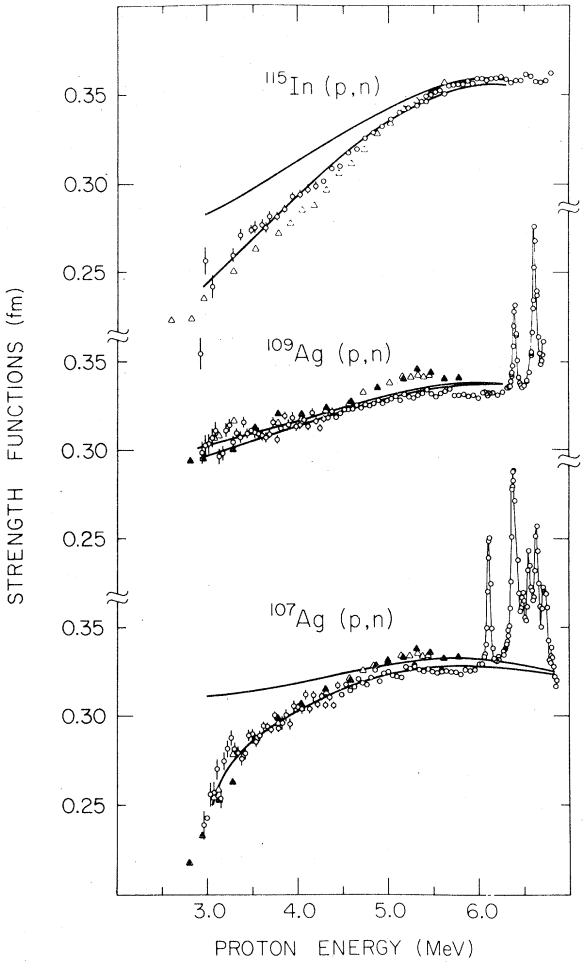

FIG. 1. Experimental and calculated strength functions. The lower curve of each set and the data represent, respectively, the calculated and experimental (p,n) strength functions. The upper curve is the calculated proton absorption strength function. The difference between each pair of curves is the calculated Hauser-Feshbach correction. The triangles (both open and solid) are data from Ref. 5.

The energy and angular dependencies of Coulomb scattering have been removed from the (p,p) data by dividing by the Rutherford cross section. The resulting ratio has been normalized to 1.0 at low energies. The (p,p) data[13] are presented in Fig. 2 where the zero of the scale has been suppressed to enhance the deviations from Rutherford scattering. Counting statistics were always less than ±0.5%.

Table II lists the uncertainties associated with the cross sections that were measured. The errors listed in Ref. 13 are counting statistical uncertainties only.

IV. OPTICAL MODEL

The optical-model potential used in this analysis is the same as that of Refs. 3 and 4. It is a conventional sum of Woods-Saxon, surface absorptive, spin-orbit, and Coulomb potentials

$$V(r)=-V_R(E)f(r,R_R,a_R)+i4a_DW_D\frac{d}{dr}f(r,R_D,a_D)$$
$$+V_{so}\frac{\vec{\sigma}\cdot\vec{l}}{r}\left(\frac{\hbar}{m_\pi c}\right)^2\frac{d}{dr}f(r,R_{so},a_{so})+V_C(R_C),$$

TABLE I. A summary of smoothed (p,n) sections.[a]

E_p [MeV]	$\sigma(p,n)$ (mb) ^{107}Ag	^{109}Ag	^{115}In[b]
3.0	0.146	0.187	0.087
3.5	0.892	1.012	0.557
4.0	3.45	3.73	2.345
4.5	10.02	10.70	7.55
5.0	23.52	24.90	19.10
5.5	46.4	49.3	41.0
6.0	81.2	84.7	75.2

[a] Interpolations can be done with the function $\exp(-37/E_p)$.

[b] ^{115}In cross sections are, in fact, natural In cross sections.

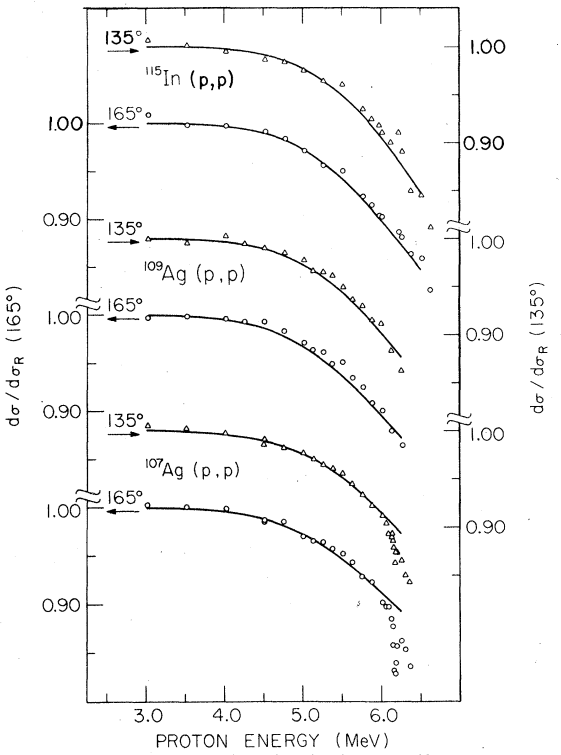

FIG. 2. Experimental and calculated differential elastic cross sections. The (p,p) data were taken at two angles for each target. The scales on the left are for 165° and the scales on the right are for 135°. The plot has been normalized by dividing by the Rutherford cross section.

where

$$f(r,R,a)=\left[1+\exp\left(\frac{r-R}{a}\right)\right]^{-1},$$

$$R_x=r_xA^{1/3},$$

$$V_R(E)=V_R(0)-b_0E,$$

$$V_R(0)=V_0+24(N-Z)/A+0.45Z/A^{1/3},$$

and V_C (R_C) is the Coulomb potential of a uniformly charged sphere of charge Ze and radius R_C.

The ten parameters of this optical-model potential are an overparametrization for the (p,n) and (p,p) data. Therefore the number of free parameters were reduced in the fitting procedure in a manner similar to Johnson *et al.*[3] For their (p,n) data, they did an investigation of the gradient of χ^2 in parameter space and fixed all but three of the most sensitive parameters. They determined that V_0, W_D, and a_D were the parameters most suited to fit the (p,n) data. A similar analysis for the (p,p) data shows that a_R, r_R, and r_D are the most sensitive parameters. Since a variation of a_R or r_R can be made to produce the same results, r_R was fixed at 1.2 fm. V_0, a_R, W_D, V_D, and a_D were varied to fit both the (p,n) and (p,p) data. The parameters $V_{so}=6.4$ MeV, $r_{so}=1.03$ fm, $a_{so}=0.63$ fm, $r_R=1.20$ fm, and $b_0=0.32$ were fixed as in Ref. 3. The r_C were fixed at 1.235, 1.233, and 1.195 fm for ^{107,109}Ag and ^{115}In, respectively. These radii were converted from the measured R_{rms} values of Ref. 14 using the relation

$$r_C=(\tfrac{5}{3})^{1/2}A^{-1/3}R_{rms}.$$

The data were fitted using the optical-model program GENOA.[15] This program does a least-squares fit to the input data and has the capability of fitting absorption and shape-elastic scattering cross sections at the same time.

V. CORRECTIONS FOR γ-RAY AND PROTON EMISSION

Although the absorption cross section is predominately the (p,n) cross section above the (p,n) threshold, near the (p,n) threshold and, to a lesser extent, at higher energies there can be a

TABLE II. Estimated uncertainties in the cross sections by source.

Source of experimental error	Standard error in $\sigma(p,n)$ (%)	Standard error in $(d\sigma/d\Omega)(p,p)$ (%)
Incident energy	±1.2 at 3 MeV ±0.5 at 6 MeV	±0.2
Energy loss in the target	±0.7 at 3 MeV ±0.3 at 6 MeV	±0.1
Charge integration	<±0.2	<±0.2
Dead time	<±0.02	<±0.2
Background and impurities	<±4.0 at 3.5 MeV <±2.0 at 4.0 MeV <±0.5 at 5.0 MeV	<±1
Counting statistics	<±1	<±0.5
Target thickness	<±2	<±1
Efficiency	<±3	

TABLE III. Fitted proton optical-model parameters.

Nucleus	V_0 (MeV)	a_R (fm)	W_D (MeV)	a_D (fm)	r_D (fm)	Source
^{107}Ag	55.0	0.80	33.0	0.34	1.35	Present work
	55.6	(0.73) [a]	22.6	0.42	(1.30) [a]	Ref. 5
^{109}Ag	55.1	0.80	32.3	0.35	1.33	Present work
	55.2	(0.73) [a]	21.3	0.42	(1.30) [a]	Ref. 5
^{115}In	53.6	0.77	17.8	0.39	1.30	Present work
	55.3	(0.73) [a]	13.9	0.41	(1.30) [a]	Ref. 5

[a] Not fitted in Ref. 5.

significant correction due to γ-ray and proton emission from the compound nucleus. To make these corrections the Hauser-Feshbach program HELGA,[16] which included γ-ray decay of the compound nucleus, was used. These corrections were made to obtain adsorption cross sections in the manner described by Johnson *et al.*[5] The γ-ray strength function parameters and level density parameters were calculated according to the prescription given by Johnson.[17] Q values were taken from Ref. 8. Low-lying levels in the target, compound, and residual nuclei were taken as the adopted values published in Nuclear Data Sheets.[18] The neutron potentials were taken from Ref. 19.

VI. DISCUSSION

The results of the simultaneous optical-model fits to the (p,n) and (p,p) data are shown in Figs. 1 and 2. In Fig. 1 the upper curve for each nuclide is the proton absorption strength function while the lower is the (p,n) strength function. The difference is the calculated Hauser-Feshbach correction for compound elastic scattering and γ-ray emission.

The parameters which correspond to the fits in Figs. 1 and 2 are presented in Table III. For comparison Table III also includes the parameters which Johnson *et al.*[5] deduced from fits to (p,n) data only. The most significant difference between the two sets of parameters is in W_D. A fit to the present (p,n) data alone shows that the resulting parameters are very close to the results of the fit to both the (p,n) and (p,p) data. Hence it is concluded that the difference in W_D is due almost entirely to the difference in curvature of the two sets of (p,n) data (Fig. 1). However, the data do agree to within the experimental accuracy. This means that the two parameter sets given in Table III from Ref. 5 and the present work represent a range in which a reasonably good fit to both the (p,n) and (p,p) data may be obtained. An attempt was also made to reduce W_D to the value used for the Sn isotopes; however, no realistic set of parameters could be found which would do this.

The (p,p) data were almost equally well fitted by either W_D in Table V and hence gives no new information about W_D. At the least the (p,p) data are consistent with the parametrization of Johnson *et al.*[5] At most it may be indicating something about the real potential parameters but, because of the redundance of a_R and r_R, the interpretation of the increase in a_R (Table III) is not clear. The elastic scattering cross section is sensitive to the nuclear size and surface diffuseness. The proton energy at which the average elastic scattering cross section deviates from Rutherford scattering measures some combination of r_R and a_R. Two speculations are that the large value of a_R is an indication of a changing rms radius or that, in reality, the large value of a_R does indicate a relatively poorly defined nuclear surface.

VII. CONCLUSIONS

The present work has shown, by an independent measurement, that the increasing value of W_D going from tin to indium to silver as reported by Johnson *et al.*[4,5] is not an artifact of their data. Furthermore, W_D is almost completely determined by the (p,n) data, i.e., the absorption cross section. The parameters which describe the (p,p) data, except for fine tuning, are essentially consistent with the (p,n) parameters. The resulting set of optical-model parameters gives a good fit to both the absorption and the elastic scattering cross sections.

The question still remains as to why the large values of W_D were required. It seems certain that in this region between closed shells there are effects which would tend to increase the absorption.[20] Whether this can be described by a coupling of the proton to states in the target in addition to the ground state or perhaps an increased density of two-particle one-hole states in the compound nuclei remains to be seen.

ACKNOWLEDGMENTS

The authors wish to thank Dr. J. P. Schiffer, Dr. R. Schrils, and Dr. M. T. McEllistrem for many helpful discussions and suggestions, Dr. G. Pepper for help with the PIXE analysis, and Dr. V. Spiegel for the loan of the National Bureau of Standards neutron source. This work was supported by the National Science Foundation.

[1]F. D. Becchetti, Jr. and G. W. Greenlees, Phys. Rev. 182, 1190 (1969).
[2]C. M. Perey and F. G. Perey, At. Data Nucl. Data Tables 17, 1 (1976).
[3] C. H. Johnson, J. K. Bair, C. M. Jones, S. K. Penny, and D. W. Smith, Phys. Rev. C 15, 196 (1977).
[4]C. H. Johnson, A. Galonsky, and R. L. Kernell, Phys. Rev. Lett. 39, 1604 (1977).
[5]C. H. Johnson, A. Galonsky, and R. L. Kernell, Phys. Rev. C 20, 2052 (1979).
[6]W. J. Courtney and J. D. Fox, At. Data and Nucl. Data Tables 15, 141 (1975).
[7]R. Schrils, D. S. Flynn, R. L. Hershberger, and F. Gabbard, Phys. Rev. C 20, 1706 (1979).
[8]A. H. Wapstra and K. Bos, At. Data Nucl. Data Tables 19, 215 (1977).
[9]R. L. Schulte, Ph.D. thesis, University of Kentucky, 1970 (unpublished).
[10]K. K. Sekharan, H. Laumer, B. D. Kern, and F. Gabbard, Nucl. Instrum. Methods 133, 253 (1976).
[11]L. F. Curtiss and A. Carson, Phys. Rev. 76, 1412 (1949); V. Spiegel (private communication).
[12]T. Teichman and E. P. Wigner, Phys. Rev. 87, 123 (1952); R. G. Thomas, *ibid.* 97, 224 (1955); Lane, Thomas, and Wigner, *ibid.* 98, 693 (1955); J. P. Schiffer and L. L. Lee, Jr., *ibid.* 109, 2098 (1958); C. H. Johnson and R. L. Kernell, Phys. Rev. C 2, 639 (1970).
[13]See AIP document No. PAPS PRVCA-21-896-8 for 8 pages of tables of cross sections. Order by PAPS number and journal reference from American Institute of Physics, Physics Auxiliary Publications Service, 335 East 45th Street, New York, New York 10017. The price is $1.50 for microfiche or $5 for photocopies. Airmail additional. Make checks payable to the American Institute of Physics. This material also appears in Current Physics Microfilm, the monthly microfilm edition of the complete set of journals published by AIP, on frames immediately following this journal article.
[14]R. C. Barrett and D. F. Jackson, *Nuclear Sizes and Structure* (Clarendon, Oxford, 1977), Chap. 6, pp. 158–159.
[15]F. G. Perey (private communication).
[16]S. K. Penny (private communication).
[17]C. H. Johnson, Phys. Rev. C 16, 2238 (1977).
[18]Nuclear Data Group, Nucl. Data Sheets, B5-5, (1971); B6-1 (1971); B7-1 (1972); 14-3 (1975); 16-2 (1975).
[19]S. A. Cox and E. E. Cox, ANL-7935 (1972) (unpublished).
[20]A. M. Lane, J. E. Lynn, E. Melkonian, and E. R. Rae, Phys. Rev. Lett. 2, 424 (1959); J. E. Lynn, *Theory of Neutron Resonance Reactions* (Clarendon, Oxford, 1968), Chap. 6, p. 280 ff.